Progress of Theoretical Physics, Vol. 90, No. 2, August 1993

Chiral Symmetry and Quark-Antiquark Pair Creation in a Strong Color-Electromagnetic Field

Hideo SUGANUMA and Toshitaka TATSUMI*,*)

RIKEN, Wako 351-01
**Department of Physics, Kyoto University, Kyoto 606-01*

(Received April 5, 1993)

We study the manifestation of chiral symmetry and q-$\bar{q}$ pair creation in the presence of the external color-electromagnetic field, using the Nambu-Jona-Lasinio model. We derive the compact formulae of the effective potential, the Dyson equation for the dynamical quark mass and the q-$\bar{q}$ pair creation rate in the covariantly constant color-electromagnetic field. Our results are compared with those in other approaches. The chiral-symmetry restoration takes place by a strong color-electric field, and the rapid reduction of the dynamical quark mass is found around the critical field strength, $\mathcal{E}_{cr} \simeq 4$ GeV/fm. Natural extension to the three-flavor case including s-quarks is also done. Around quarks or antiquarks, chiral symmetry would be restored by the sufficiently strong color-electric field, which may lead to the chiral bag picture of hadrons. For the early stage for ultrarelativistic heavy-ion collisions, the possibility of the chiral-symmetry restoration is indicated in the central region just after the collisions.

§ 1. Introduction

In recent years, many studies have been devoted to clarifying the structure of hadrons and the properties of the nonperturbative vacuum in the low-energy realm of QCD. As is well-known, there are two outstanding features; the spontaneous breaking of chiral symmetry (χSB) and the color confinement. In particular, much interest has been paid to the manifestation of chiral symmetry to analyze the nonperturbative QCD vacuum and related hadron features by way of the effective models of QCD[1)~3)] or lattice QCD simulations:[4)] theoretically the chiral-symmetry restoration in various circumstances has been studied, e.g., at high temperature or in high density matter;[5)] phenomenologically this phase transition has been expected in quark-gluon-plasma (QGP) formations[6)] or in hadronic matter[7)] inside dense stars. Although many important aspects have been revealed by these studies, most analyses, except for lattice QCD simulations, have been done mainly based on the quark degrees of freedom, and the gluon contribution is included at most up to the lowest order of the perturbation as one-gluon exchange effect.

The symmetry restoration at high temperature or in high-density matter is a phase transition from the Nambu-Goldstone (NG) phase to the Wigner-Weyl (WW) one and we can expect similar situation in the (color-)electromagnetic (EM) field.[8)~12)] In distinction from the former case, the latter one needs no 'coarse graining' and is important not only for the phase transition but also for hadron structure; hadrons consist of valence quarks and/or antiquarks, which exert a strong color-EM field as color sources and in turn may alter the property of the QCD vacuum around them.

*) Present address: Institut für Theoretische Physik, Universität Heidelberg, Philosophenweg 19, D-6900, Heidelberg, Germany.

Actually, some lattice QCD simulations indicate that chiral symmetry is restored in the vicinity of quarks.[13]

In the preceding studies,[8),11)] restoration of chiral symmetry in a strong electric field has been discussed and we have seen that the quark condensate or the σ field, which should be an order parameter of chiral symmetry, is washed away by a strong electric field at the critical strength $eE_c \simeq (480\,\mathrm{MeV})^2$. One hardly obtains such a strong field as it is in the nature. Moreover, strictly speaking chiral symmetry is *always* broken explicitly there by the electric field since it couples with the electric charges of quarks, which breaks the isospin symmetry.

In this paper, we treat the manifestation of chiral symmetry in the presence of the strong external color-EM field. In difference from the QED case just mentioned above, one can expect a very strong color-EM field around quarks.*) Moreover it never breaks chiral symmetry explicitly since its coupling with quarks does not depend on the flavor degree of freedom. Thus the strong color field is compatible with chiral symmetry.

In the low-energy region, QCD is very difficult to investigate analytically, so that one is obliged to use some elaborate numerical methods or effective models. Direct calculations like lattice QCD simulations[4)] have been proved to be powerful, but there are some technical limits at present and it seems hard to extract physics included in their results. We believe that some effective-model approaches[1)~3),14)] should be indispensable to deeply understand the low-energy realm of QCD in parallel with such numerical methods. Here we use the Nambu-Jona-Lasinio (NJL) model, to study our subject, which has been frequently used to study the manifestation of chiral symmetry.[2)] We would like to give some remarks on our approach. The NJL model may be considered as an effective field theory, which describes the intermediate region between confinement scale Λ_{QCD} and the χSB scale $\Lambda_{\chi\mathrm{SB}}$. The idea of intermediate region has been given by Manohar and Georgi,[1)] and this provides an understanding of the successes of the non-relativistic quark model and the physical meaning of massive constituent quarks. In this region the quark-gluon interaction will still be described by an $SU(3)_c$ gauge theory, while there scarcely exist nonperturbative effects relevant to the confinement like the gluon condensate,[15),16)] for which the self-interaction of gluons is essential. On the other hand, nonperturbative effects relevant to the χSB may survive even in the intermediate region. The NJL model is different from the chiral quark model by Manohar and Georgi in the treatment of the constituent-quark mass and the Goldstone bosons. Constituent quark mass, which is introduced by hand in their chiral quark model, is dynamically generated by the attractive four-fermion interaction in the NJL model. The NJL model naturally includes pseudoscalar Goldstone bosons as collective states of $\bar{q}q$ pair in place of fundamental fields. We shall adopt this picture and concentrate on the manifestation of chiral symmetry in this intermediate region in what follows.

Since the quark condensate, $\langle \bar{q}q \rangle$, which is the order parameter of spontaneous chiral-symmetry breaking and is given by the trace of the quark propagator, is colorless, it cannot couple to the external color-EM field directly, but does only

*) In § 6, we shall see that sufficiently strong color-EM field would appear inside hadrons or in relativistic heavy-ion collisions.

through the quantum fluctuations given by loops of colored particles. Then analysis at the quantum level is indispensable in our subject. It is useful to apply the effective potential approach[8),9),17)] in analyzing the manifestation of symmetry in external fields, because the quantum fluctuations can be incorporated and the intuitive physical insight can be obtained by way of it. In the presence of the external color-EM field, not only the chiral-symmetry phase transition but also quark and antiquark (q-$\bar{q}$) pair creation can take place by the Schwinger mechanism[18),19)] similar to e^+-e^- pair creation in QED. In recent years, q-$\bar{q}$ creation has been also studied with vigor in the context of QGP formation in ultrarelativistic heavy-ion collisions,[19)] where a strong color field is expected in their early stage. Then it is desirable to incorporate q-$\bar{q}$ pair creation in the study of chiral symmetry in the color-EM field. In the theoretical point of view, these two phenomena are much related in terms of the effective potential; its real part determines the manifestation of chiral symmetry or the dynamical quark mass, on the other hand its imaginary part implies q-$\bar{q}$ pair creation.[9),20)] Hence we study these phenomena simultaneously and their relation in terms of the effective potential. Since quark condensate $\langle\bar{q}q\rangle$ is given by the trace of the quark propagator G_q, $\langle\bar{q}q\rangle=(1/i)\mathrm{Tr}G_q$, and the $\bar{q}$-q pair creation rate is given by $w \propto \mathrm{Im}((1/i)\mathrm{Tr}\ln G_q)$ (see (2·26)), quark loop is the primary ingredient in our context.*) We shall take the NJL model with the coupling to the external color-EM field as one of the suitable models in studying these subjects.

The effective potential will be evaluated by way of the proper-time method to compare our approach with another one based on the constrained Hartree approximation adopted by Klevansky et al. in a similar context.[11),12)] Of course we can use the ζ-function regularization method as an alternative, which has been a useful method to study quantum effects in QED.[17),21)] Hence we shall briefly discuss the relationship and differences between them in the Appendix.

In § 2, we present our approach and derive the effective potential in the presence of the external color-EM field. The Dyson equation of quarks can be derived by taking the extremum of the real part of the effective potential. The q-$\bar{q}$ pair creation rate is derived from its imaginary part. In § 3, we illustrate our theory by giving some numerical examples for the system around quarks. In § 4, we extend the theory to the three-flavor case including s-quark, and calculate the physical quantities related to the strangeness. In § 5, the effective potential approach is compared with another approach based on the constrained Hartree approximation. In § 6, we discuss the hadron structure in terms of the color-electric flux tube picture. We also study the pre-equilibrium stage of the ultrarelativistic heavy-ion collisions there. Section 7 is devoted to a summary and concluding remarks.

§ 2. Formalism

In this section, we study the manifestation of chiral symmetry in the intermediate region between the confinement and the χSB scales using the NJL model, when the

*) The gluon loops, on the other hand, should play an essential role for the confinement.

system is immersed in the external color-EM field. The effective Lagrangian is expressed by quarks (q^a) and gluons ($G^\mu = G^{\mu a} T^a$),*)

$$\mathcal{L} = \mathcal{L}_{\rm NJL}[q, \bar{q}] + g j_\mu^a G^{\mu a} - \frac{1}{2}{\rm tr}_c(\mathcal{F}^{\mu\nu}\mathcal{F}_{\mu\nu}) ; \tag{2·1}$$

where $\mathcal{F}_{\mu\nu} = \partial_\mu G_\nu - \partial_\nu G_\mu - ig[G_\mu, G_\nu]$ is the field strength of gluons and ${\rm tr}_c$ means the trace over the color space; $j_\mu^a = \bar{q}\gamma_\mu T^a q$ is the color current of the quark which couples to gluons; $\mathcal{L}_{\rm NJL}$ is the ordinary NJL Lagrangian,

$$\mathcal{L}_{\rm NJL}[q, \bar{q}] = \bar{q}(i\partial\!\!\!/ - \bar{m})q + g_{\rm NJL}[(\bar{q}q)^2 + (\bar{q}i\gamma_5 \boldsymbol{\tau} q)^2] , \tag{2·2}$$

where $\bar{m} = (m_u + m_d)/2$ is the averaged current mass of u, d-quarks. Since nonperturbative effects relevant to the χSB should be considered to be already included in the four-fermion interaction among quarks, we do not explicitly take into account gluon dynamics neglecting their internal lines in Feynman diagrams. Then only the diagrams including the external-gluon lines remain relevant, so that we hereafter will drop the kinetic term of gluons. The following is to be noted. Nonperturbative effects relevant to the confinement like the gluon condensate scarcely exist in the intermediate region, so that it is no more necessary to consider the coupling of the external gluon field with them.

Current quarks are considered to get large mass (constituent quark mass) by the dynamical effects and turn into the constituent quarks in the intermediate region. This dynamical effect leads to the χSB, which is one of the most outstanding features in the low-energy realm of QCD; such a mechanism is incorporated in the NJL model. Lagrangian (2·1) has chiral symmetry, $SU(2)_L \times SU(2)_R$, except for the small current-quark mass term.**) In the physical state with no external fields, however, this symmetry is spontaneously broken into $SU(2)_V$, because quarks get a large dynamical mass due to the attractive four-fermion interaction between them. Therefore the dynamical quark mass should vary according to the circumstance, such as at high temperature, in high density or in the strong (color-)EM field.

By using auxiliary fields σ and $\boldsymbol{\pi}$, Lagrangian (2·2) can be equivalently expressed as

$$\mathcal{L}_{\rm aux}[q, \bar{q}, \sigma, \boldsymbol{\pi}] = \bar{q}(i\partial\!\!\!/ - \bar{m})q - \bar{q}(\sigma + i\gamma_5 \boldsymbol{\tau}\cdot\boldsymbol{\pi})q - \frac{1}{4g_{\rm NJL}}(\sigma^2 + \boldsymbol{\pi}^2) . \tag{2·3}$$

Hence the partition functional $Z[J_\sigma, \boldsymbol{J}_\pi]$ is given by

$$Z[J_\sigma, \boldsymbol{J}_\pi] = \int \mathcal{D}q \mathcal{D}\bar{q} \mathcal{D}\sigma \mathcal{D}\boldsymbol{\pi} \exp\left\{ i \int d^4x (\mathcal{L}_{\rm aux}[q, \bar{q}, \sigma, \boldsymbol{\pi}] + g j_\mu^a G_{\rm ex}^{\mu a} + J_\sigma \sigma + \boldsymbol{J}_\pi \cdot \boldsymbol{\pi}) \right\} , \tag{2·4}$$

*) The symbol T^a ($a = 1, 2, \cdots, 8$) denotes the generators of gauge symmetry $SU(3)_c$, while we will use the symbol $\lambda^a/2$ for those of flavor symmetry $SU(3)_f$.

**) An extension to the three-flavor case will be done in § 4.

where $G_{\rm ex}^{\mu a}$ is an external gluon field; $J_\sigma\sigma$ and $\boldsymbol{J}_\pi\cdot\boldsymbol{\pi}$ are the source terms.*) Then the quark condensate $\langle\bar{q}q\rangle_J$ and the vacuum expectation value $\langle\sigma\rangle_J$ are related with each other:

$$\langle\bar{q}q\rangle_J=-\frac{1}{2g_{\rm NJL}}\langle\sigma\rangle_J+J_\sigma=-\frac{1}{2g_{\rm NJL}}\frac{1}{iZ}\frac{\delta Z}{\delta J_\sigma}+J_\sigma\,, \tag{2·5}$$

in the presence of the source term, so that $\langle\bar{q}q\rangle_J$ is not simply proportional to $\langle\sigma\rangle_J$ except for $J_\sigma=0$.

After the functional integration over the quark field in Eq. (2·4), one obtains the effective Lagrangian of σ and $\boldsymbol{\pi}$,

$$\mathcal{L}_{\rm eff}[\sigma,\boldsymbol{\pi}]=-\frac{1}{4g_{\rm NJL}}(\sigma^2+\boldsymbol{\pi}^2)+\mathcal{L}_{\rm loop}[\sigma,\boldsymbol{\pi}] \tag{2·6}$$

in the mean-field approximation for σ and $\boldsymbol{\pi}$; $\mathcal{L}_{\rm loop}$ denotes the loop effect of quarks,

$$\mathcal{L}_{\rm loop}[\sigma,\boldsymbol{\pi}]=-i{\rm Tr}\ln\{(i\partial\!\!\!/+g\mathcal{G}_{\rm ex})-(\bar{m}+\sigma+i\gamma_5\boldsymbol{\tau}\cdot\boldsymbol{\pi})+i\epsilon\}\,. \tag{2·7}$$

In Eq. (2·7), Tr means the functional trace over the quark degrees of freedom, i.e., the coordinate space, spin, flavor and color indices. We are interested in the system with translational invariance, so that σ and $\boldsymbol{\pi}$ are constant and the effective Lagrangian $\mathcal{L}_{\rm eff}$ is reduced to

$$\mathcal{L}_{\rm eff}[\sigma,\boldsymbol{\pi}]$$
$$=-\frac{1}{4g_{\rm NJL}}(\sigma^2+\boldsymbol{\pi}^2)-\frac{i}{2}{\rm Tr}\ln\left\{-(i\partial^\mu+gG_{\rm ex}^\mu)^2-\frac{g}{2}\sigma_{\mu\nu}\mathcal{F}_{\rm ex}^{\mu\nu}+\bar{M}^2+\boldsymbol{\pi}^2-i\epsilon\right\}, \tag{2·8}$$

where $\bar{M}\equiv\bar{m}+\sigma$ is the dynamical quark mass and $\sigma_{\mu\nu}=-(i/2)[\gamma_\mu,\gamma_\nu]$.

Now we consider the case where the external field is covariantly constant,[15),22)] that is to say, the covariant derivative ($\mathcal{D}_\mu=\partial_\mu-igG_\mu$) and the field strength commutes,**)

$$[\mathcal{D}_\mu,\mathcal{F}_{\alpha\beta}]=0\,. \tag{2·9}$$

This is a natural extension of the constant field condition in QED to the non-abelian gauge theory, and guarantees *translational invariance* of the system[23)] (see Eq. (2·14)). Due to the Jacobi identity,

$$[[\mathcal{D}_\mu,\mathcal{D}_\nu],\mathcal{F}_{\alpha\beta}]+[[\mathcal{D}_\nu,\mathcal{F}_{\alpha\beta}],\mathcal{D}_\mu]+[[\mathcal{F}_{\alpha\beta},\mathcal{D}_\mu],\mathcal{D}_\nu]=0\,, \tag{2·10}$$

and the general relation $[\mathcal{D}_\mu,\mathcal{D}_\nu]=-ig\mathcal{F}_{\mu\nu}$, one finds that the $\mathcal{F}_{\mu\nu}$'s commute with each other,

$$[\mathcal{F}_{\mu\nu},\mathcal{F}_{\alpha\beta}]=0\,. \tag{2·11}$$

Hence, all of the $\mathcal{F}_{\mu\nu}$'s ($\mu,\nu=0,1,2,3$) can be diagonalized simultaneously in a suitable representation, e.g., in a fundamental representation of $SU(3)_c$,

*) The introduction of the source terms is not unique for the composite order parameter. Another type of the source terms will be discussed in § 5.

**) We hereafter drop the subscript "ex" in the symbols, $G_{\rm ex}^\mu$ and $\mathcal{F}_{\rm ex}^{\alpha\beta}$.

$$\mathcal{F}_{\mu\nu}=\mathrm{diag}(\mathcal{F}^{(1)}_{\mu\nu}, \mathcal{F}^{(2)}_{\mu\nu}, \mathcal{F}^{(3)}_{\mu\nu})_c=\mathcal{F}^{A}_{\mu\nu}T^3+\mathcal{F}^{B}_{\mu\nu}T^8 . \tag{2·12}$$

By the condition (2·9), the group structure for the external field is altered from $SU(3)_c$ to its maximal torus subgroup $U(1)_A\times U(1)_B$; there appears two kinds of charge expressed by Q_A and Q_B according to $U(1)_A$ and $U(1)_B$, respectively.[24),*] Moreover, by choosing a suitable gauge, gluons G_μ can be simply expressed in the diagonal form,

$$G^\mu=-\frac{1}{2}\mathcal{F}^{\mu\nu}x_\nu , \tag{2·13}$$

so that one also finds

$$[G_\mu, \mathcal{F}_{\alpha\beta}]=0 , \quad [\partial_\mu, \mathcal{F}_{\alpha\beta}]=0 . \tag{2·14}$$

Then $\mathcal{F}_{\mu\nu}$ $(\mu, \nu=0, 1, 2, 3)$ are independent of the space-time coordinate x_μ in this gauge. Due to Eqs. (2·9) and (2·11), similar formulae and parallel arguments to QED or the abelian case can be applied in this case.[8] Taking a suitable Lorentz frame, $\mathcal{F}^{(i)}_{\mu\nu}$ $(i=1, 2, 3)$, diagonal element of $\mathcal{F}_{\mu\nu}$, can be chosen as follows without loss of generality,**)

$$E^{(i)}=\mathcal{F}^{(i)}_{03}=-\mathcal{F}^{(i)}_{30}(\geq 0), H^{(i)}=\mathcal{F}^{(i)}_{12}=-\mathcal{F}^{(i)}_{21}(\geq 0), \mathcal{F}^{(i)}_{\mu\nu}=0 \text{ (others)} . \tag{2·15}$$

By way of the proper-time method,[26] the logarithm of an operator $\hat{O}$ can be expressed by

$$\ln\hat{O}=-\int_0^\infty \frac{d\tau}{\tau}e^{-i\tau\hat{O}} \tag{2·16}$$

apart from irrelevant constant. Hence after some calculation, one can obtain the compact expression for $\mathcal{L}_{\text{loop}}$,

$$\begin{aligned}\mathcal{L}_{\text{loop}}&=-\frac{N_f}{8\pi^2}\mathrm{tr}_c\int_0^\infty \frac{d\tau}{\tau^3}e^{-i\tau(\bar{M}^2+\boldsymbol{\pi}^2-i\epsilon)}(gE\tau)\coth(gE\tau)\cdot(gH\tau)\cot(gH\tau)\\ &=-\frac{N_f}{8\pi^2}\mathrm{tr}_c\mathrm{pv}\int_0^\infty \frac{ds}{s^3}e^{-s(\bar{M}^2+\boldsymbol{\pi}^2)}(gEs)\cot(gEs)\cdot(gHs)\coth(gHs)\\ &\quad+i\frac{N_f}{8\pi^2}\mathrm{tr}_c\sum_{n=1}^{\infty}\frac{gH\cdot gE}{n}\coth(HE^{-1}n\pi)\exp\{-n\pi(\bar{M}^2+\boldsymbol{\pi}^2)/(gE)\} ,\end{aligned} \tag{2·17}$$

where "pv" means the principal value. Here we have modified the integral path and changed the variable τ into $s\equiv i\tau$ in Eq. (2·17). The imaginary part in $\mathcal{L}_{\text{eff}}$ originates from the poles at $\tau=-in\pi/(gE)$ in the complex τ-plane.

The integral in the second line in Eq. (2·17) diverges at $s=0$ that corresponds to the high-energy limit. This divergence originates from the loop integral over the quark field, and should be removed by the renormalization procedure. Unfortunate-

*) This subgroup is suggested to be relevant in the abelian projection scheme of QCD, in which the diagonal parts of the nonabelian gauge field may be largely responsible to the quark confinement.[25]

**) In a general Lorentz frame, H and E are described in terms of two Lorentz invariants $\mathcal{F}$ and $\mathcal{G}$: $H, E=[(\mathcal{F}^2+\mathcal{G}^2)^{1/2}\pm\mathcal{F}]^{1/2}$, where $\mathcal{F}=(1/4)\mathcal{F}_{\mu\nu}\mathcal{F}^{\mu\nu}$, $\mathcal{G}=(1/4)\mathcal{F}_{\mu\nu}\tilde{\mathcal{F}}^{\mu\nu}$.

ly, the NJL model is, however, non-renormalizable, so that ad hoc regularization is needed to extract meaningful finite results.*) Since the NJL model is an effective model, it is reasonable to introduce a ultra-violet cutoff Λ and avoid the ultra-violet divergence at $s=0$: the lower bound in the s-integral should be replaced by $1/\Lambda^2$.**)

Then the effective potential for σ and $\boldsymbol{\pi}$ is given by

$$V_{\rm eff}=-\mathcal{L}_{\rm eff}=\frac{(\bar{M}-\bar{m})^2+\boldsymbol{\pi}^2}{4g_{\rm NJL}}$$
$$+\frac{N_f}{8\pi^2}{\rm tr}_c{\rm pv}\int_{1/\Lambda^2}^{\infty}\frac{ds}{s^3}e^{-s(\bar{M}^2+\pi^2)}(gEs)\cot(gEs)\cdot(gHs)\coth(gHs)$$
$$-i\frac{N_f}{8\pi^2}{\rm tr}_c\sum_{n=1}^{\infty}\frac{gH\cdot gE}{n}\coth(HE^{-1}n\pi)\exp\{-n\pi(\bar{M}^2+\boldsymbol{\pi}^2)/(gE)\}\,, \qquad (2\cdot18)$$

because of the absence of the kinetic terms of σ and $\boldsymbol{\pi}$. It is notable that the full order of gE or gH is incorporated in Eq. (2·17). In particular, the imaginary part of $V_{\rm eff}$ is purely nonperturbative effects of gE: it cannot be obtained by the perturbation of any finite order of gE. The physical meaning of the effective potential is as follows; its real part corresponds to the energy of the vacuum, and its imaginary part expresses the instability of the vacuum against q-$\bar{q}$ pair creation. Then the physical vacuum is determined by the real part of the effective potential $V_{\rm eff}$, while its imaginary part gives the q-$\bar{q}$ pair creation rate per unit time-space volume (the Schwinger mechanism).[20]

Then the physical values of σ and $\boldsymbol{\pi}$ in the presence of the external color-EM field are determined by minimizing the *real part* of the effective potential $V_{\rm eff}$,

$$\frac{\partial}{\partial\sigma}{\rm Re}\,V_{\rm eff}(\sigma,\boldsymbol{\pi})=0\,,\quad \frac{\partial}{\partial\boldsymbol{\pi}}{\rm Re}\,V_{\rm eff}(\sigma,\boldsymbol{\pi})=0\,. \qquad (2\cdot19)$$

Due to the explicit breaking of chiral symmetry, one obtains $\boldsymbol{\pi}=0$.***) Therefore one obtains the self-consistent Dyson equation for the dynamical quark mass $\bar{M}_D$ in the external field,

$$\bar{M}_D=\bar{m}+\frac{N_f g_{\rm NJL}}{2\pi^2}\bar{M}_D{\rm tr}_c{\rm pv}\int_{1/\Lambda^2}^{\infty}\frac{ds}{s^2}e^{-s\bar{M}_D^2}(gEs)\cot(gEs)\cdot(gHs)\coth(gHs)$$
$$=\bar{m}+\frac{N_f g_{\rm NJL}}{2\pi^2}\bar{M}_D N_c\int_{1/\Lambda^2}^{\infty}\frac{ds}{s^2}e^{-s\bar{M}_D^2}$$
$$-\frac{N_f g_{\rm NJL}}{2\pi^2}\bar{M}_D g\sum_{i=1}^{3}F_{\eta^{(i)}}^{\rm fermion}(x^{(i)},\theta^{(i)})\cdot(H^{(i)2}+E^{(i)2})^{1/2}\,, \qquad (2\cdot20)$$

where

*) Hence the results generally depend on the way of regularization. See the discussion given in § 5 and the Appendix.

**) We use this prescription in the lower formula in Eq. (2·17). If one uses this in the upper formula, there appear some difficulties in eliciting the imaginary part.

***) In chiral limit, however, $\boldsymbol{\pi}=0$ cannot be derived by such an energetical argument, because all points in the chiral circle "$\sigma^2+\boldsymbol{\pi}^2=$const" degenerate. Hence one has to impose $\boldsymbol{\pi}=0$ as the physical requirement.

$$F_\eta^{\text{fermion}}(x,\theta)\equiv -\text{pv}\int_\eta^\infty \frac{ds}{s^2}e^{-sx^2}[(s\cos\theta)\coth(s\cos\theta)\cdot(s\sin\theta)\cot(s\sin\theta)-1] \tag{2·21}$$

is a characteristic function,

$$H=\text{diag}(H^{(1)},H^{(2)},H^{(3)})_c\,,\quad E=\text{diag}(E^{(1)},E^{(2)},E^{(3)})_c\,,$$
$$x^{(i)}=\bar{M}_D/\{(gE^{(i)})^2+(gH^{(i)})^2\}^{1/4}\,,\quad \theta^{(i)}=\arctan(E^{(i)}/H^{(i)})\,,$$
$$\eta^{(i)}=g(H^{(i)2}+E^{(i)2})^{1/2}/\Lambda^2\,. \tag{2·22}$$

Since the value of Λ is large, $F_\eta^{\text{fermion}}(x,\theta)$ behaves quite similarly to

$$F^{\text{fermion}}(x,\theta)\equiv F_{\eta=0}^{\text{fermion}}(x,\theta) \tag{2·23}$$

in the interesting region of H or E, where the chiral-symmetry restoration occurs. The behavior of chiral symmetry is indicated by the sign of the characteristic function (2·21): if $F^{\text{fermion}}>0$, chiral symmetry tends to be restored, while its breaking tends to be enhanced if $F^{\text{fermion}}<0$. The properties of $F^{\text{fermion}}(x,\theta)$ are fully discussed in Ref. 8), and its behavior is shown in Fig. 1. We briefly summarize here the contribution of each component (i) of the color-EM field to the manifestation of chiral symmetry: typically, in the purely color-magnetic case ($\theta=0$) one gets $F^{\text{fermion}}<0$, the χSB is enhanced and $\bar{M}_D$ increases; on the contrary, in the purely color-electric case ($\theta=\pi/2$) one gets $F^{\text{fermion}}>0$, chiral symmetry tends to be restored and $\bar{M}_D$ decreases. Quantitatively, the latter tendency is more remarkable than the former one. It comes from the fact that x decreases rapidly for the color-electric field, while x varies moderately for the color-magnetic field (see Eq. (2·22) and Fig. 1).

From Eq. (2·20), one can derive the simple relation for the critical color-electric

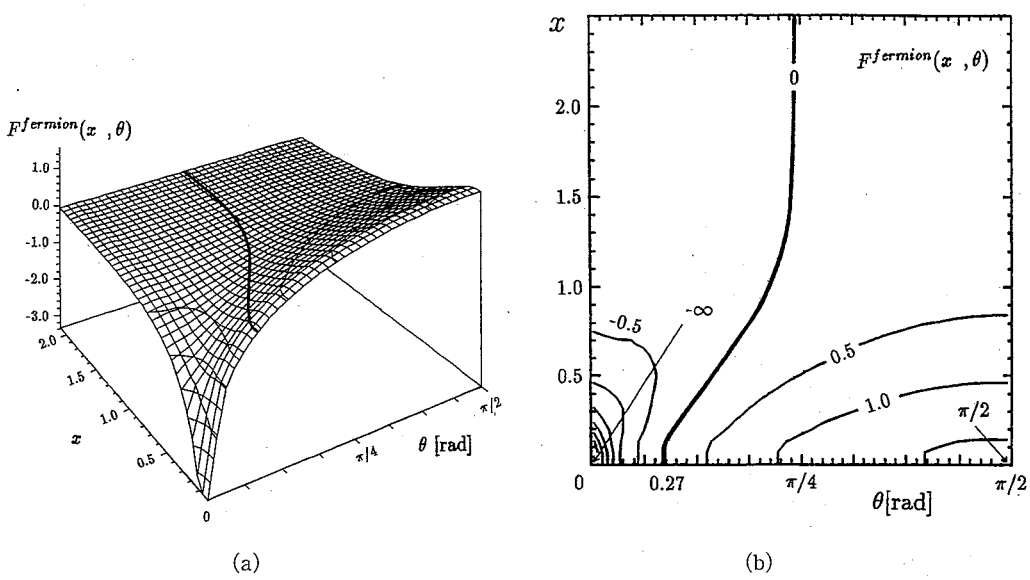

(a) (b)

Fig. 1. (a) Global shape of the characteristic function, $F^{\text{fermion}}(x,\theta)$ and (b) its contour map. Positive-valued region of $F^{\text{fermion}}(x,\theta)$ increases for small x, corresponding to the strong color-EM field.

field $E_{\rm cr}^{(i)}$ of the chiral-symmetry restoration ($x^{(i)}=0$),

$$N_c\Lambda^2-\frac{2\pi^2}{N_f g_{\rm NJL}}\simeq\sum_{i=1}^{3}gE_{\rm cr}^{(i)}\cdot F^{\rm fermion}(0,\,\theta^{(i)})/\sin\theta^{(i)}$$

$$=\sum_{i=1}^{3}gE_{\rm cr}^{(i)}\cdot 2\pi\left[\frac{1}{4}-\sum_{n=1}^{\infty}\frac{1}{e^{2n\pi\tan\theta^{(i)}}-1}\right] \qquad (2\cdot24)$$

in the chiral limit ($\bar{m}=0$). Thus the critical color-electric field is characterized by the combination $f(\theta^{(i)})\equiv\sin\theta^{(i)}/F^{\rm fermion}(0,\,\theta^{(i)})$. For a large color-EM field ($x^{(i)}\simeq 0$), each (i)-component contributes to the symmetry restoration as long as $F^{\rm fermion}(0,\,\theta^{(i)})$ is positive, which corresponds to $\theta^{(i)}>0.27$ or $H^{(i)}<3.6E^{(i)}$ (see Fig. 1). Here the color-magnetic field hardly disturbs the symmetry restoration at least for $H^{(i)}\lesssim E^{(i)}$, i.e., $\theta^{(i)}\gtrsim\pi/4$, for instance, one finds

$$f(\theta^{(i)}=\pi/4)\simeq 1.008\cdot f(\theta^{(i)}=\pi/2)\,. \qquad (2\cdot25)$$

On the other hand, the *imaginary part* of the effective potential means q-$\bar{q}$ pair creation; its rate per unit time-space volume w is related to the vacuum persistency amplitude,

$$e^{-w\int d^4x}=|\langle{\rm out}|{\rm in}\rangle|^2=e^{-2{\rm Im}\mathcal{L}_{\rm eff}\int d^4x}\,, \qquad (2\cdot26)$$

so that one obtains

$$w(\bar{M}_D)=2{\rm Im}\mathcal{L}_{\rm eff}=-2{\rm Im}\,V_{\rm eff}$$

$$=\frac{N_f}{4\pi^2}{\rm tr}_c\sum_{n=1}^{\infty}\frac{gH\cdot gE}{n}\coth(HE^{-1}n\pi)\exp\{-n\pi\bar{M}_D{}^2/(gE)\}\,, \qquad (2\cdot27)$$

which is reduced to

$$w(\bar{M}_D)=\frac{N_f}{4\pi^3}{\rm tr}_c\sum_{n=1}^{\infty}\frac{(gE)^2}{n^2}e^{-n\pi\bar{M}_D{}^2/(gE)} \qquad (2\cdot28)$$

in a particular case $H=0$.

§ 3. Numerical examples

We consider some physical situations and examine the manifestation of chiral symmetry and the q-$\bar{q}$ pair creation rate around the quark, where the external gluon field would be locally uniform and is covariantly constant within the static approximation.

In a suitable representation of $SU(3)_c$, the color charges of the red, blue and green quarks are given by

$$(Q_A,\,Q_B)=\left(\frac{1}{2}g,\,\frac{1}{2\sqrt{3}}g\right),\left(-\frac{1}{2}g,\,\frac{1}{2\sqrt{3}}g\right),\left(0,\,-\frac{1}{\sqrt{3}}g\right), \qquad (3\cdot1)$$

respectively.[24] Since the diagonal components of E, E_A and E_B, are given by the color charges Q_A and Q_B, respectively, $(E_A,\,E_B)$ is expected to be proportional to $(Q_A,\,Q_B)$. Hence one obtains the color-electric field around the quark, e.g. red quark, gE

$=\sqrt{(gE_AT^3+gE_BT^8)^2}=\mathrm{diag}(\mathcal{E}/3,\ \mathcal{E}/6,\ \mathcal{E}/6)_c$, where $\mathcal{E}\equiv\sqrt{3}g(E_A{}^2+E_B{}^2)^{1/2}$.

Hence the effective potential $V_{\rm eff}$ around a given color quark leads to

$$\mathrm{Re}\,V_{\rm eff}=\frac{(\bar{M}-\bar{m})^2}{4g_{\rm NJL}}+\frac{N_f}{8\pi^2}\mathrm{pv}\int_{1/\Lambda^2}^{\infty}\frac{ds}{s^3}e^{-s\bar{M}^2}\left[\left(\frac{\mathcal{E}}{3}s\right)\cot\left(\frac{\mathcal{E}}{3}s\right)+2\left(\frac{\mathcal{E}}{6}s\right)\cot\left(\frac{\mathcal{E}}{6}\right)\right],$$

$$\mathrm{Im}\,V_{\rm eff}=-\frac{N_f}{8\pi^3}\sum_{n=1}^{\infty}\frac{1}{n^2}\left[\left(\frac{\mathcal{E}}{3}\right)^2\exp\left\{-\frac{3}{\mathcal{E}}\bar{M}^2n\pi\right\}+2\left(\frac{\mathcal{E}}{6}\right)^2\exp\left\{-\frac{6}{\mathcal{E}}\bar{M}^2n\pi\right\}\right] \quad (3\cdot2)$$

independent of the color. Note that two terms appear in the brackets in Eq. (3·2) due to two kinds of charge (if one uses $U(1)$ approximation to the external 'color' field, only one term appears[8),12)]).

Here we choose the following parameter sets,

(i) the empirical case ($\bar{m}=(m_u+m_d)/2\simeq5.5$ MeV): $g_{\rm NJL}=0.211$ fm^2, $\Lambda=950$ MeV.

(ii) the chiral limit ($\bar{m}=0$); $g_{\rm NJL}=0.214$ fm^2, $\Lambda=950$ MeV.

These values have been selected so that they give the empirical values of the quark condensate and the constituent quark mass,

$$\langle\bar{u}u\rangle=\langle\bar{d}d\rangle=-(250\ \mathrm{MeV})^3,\quad \bar{M}_D=335\ \mathrm{MeV} \quad (3\cdot3)$$

in the absence of the external field. In both cases (i) and (ii), the pion decay constant f_π is expressed by

$$f_\pi{}^2=\frac{N_c}{4\pi^2}\bar{M}_D{}^2\int_{1/\Lambda^2}^{\infty}\frac{ds}{s}e^{-s\bar{M}_D{}^2}\simeq(118\ \mathrm{MeV})^2 \quad (3\cdot4)$$

for $H=E=0$. The variations of the real and imaginary parts of $V_{\rm eff}$ as $\mathcal{E}$ increases

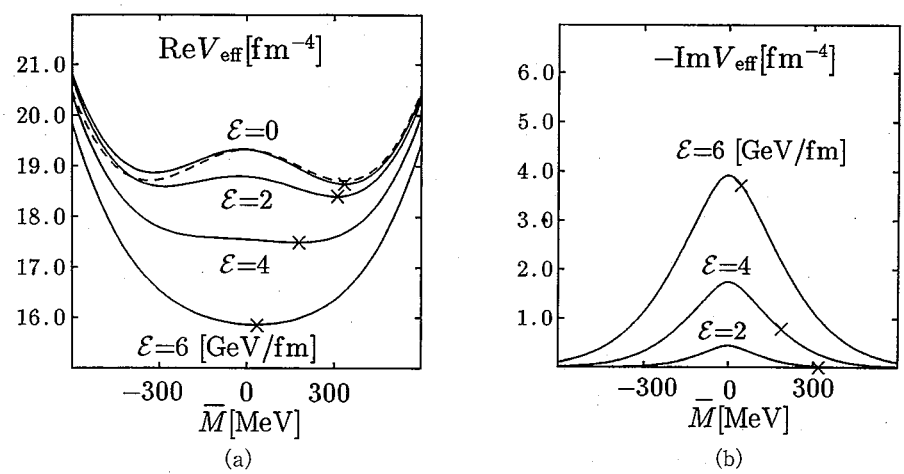

Fig. 2. (a) Real part and (b) imaginary part of the effective potential $V_{\rm eff}$ in the presence of the external color-EM field as functions of the quark mass $\bar{M}$. The solid lines correspond to the empirical case ($\bar{m}=5.5$ MeV) for $\mathcal{E}=0$, 2, 4, 6 GeV/fm. The absolute minimum of Re $V_{\rm eff}$ (physical vacuum) is indicated by cross $\times$. The broken line corresponds to the chiral limit ($\bar{m}=0$) in the absence of the external field. Cross $\times$ in (b) corresponds to the physical vacuum for the empirical case.

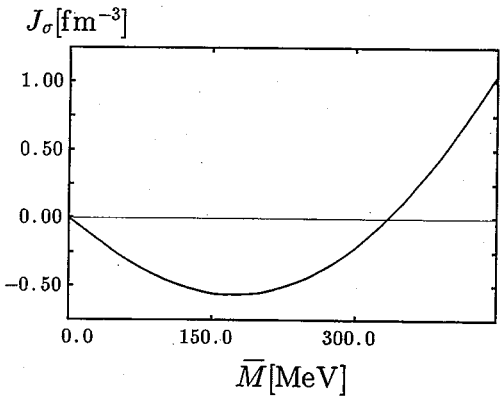

Fig. 3. Variation of the source J_σ in the absence of the color-EM field (the chiral limit). The horizontal axis denotes $\bar{M}$. The source J_σ takes a non-vanishing value except for the extrema of Re $V_{\rm eff}$.

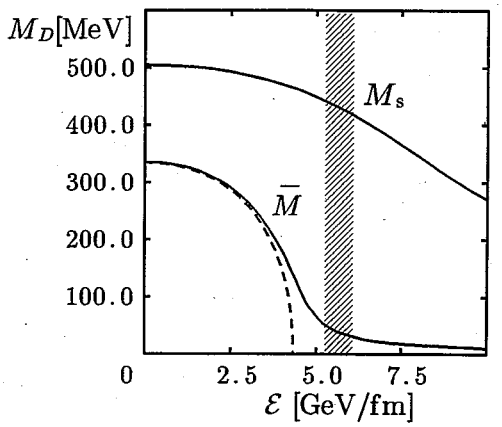

Fig. 4. Dynamical quark masses as functions of $\mathcal{E}$. The lower two lines express the variable for u, d-quarks: the solid and dashed lines correspond to (i) the empirical case ($\bar{m}$=5.5 MeV) and (ii) the chiral limit ($\bar{m}$=0), respectively. The upper solid line expresses the variable for s-quarks. The shaded region corresponds to the "empirical" value of $\mathcal{E}$ inside hadrons ($\mathcal{E}$=5.3 ~6 [GeV/fm]).

are shown in Figs. 2(a) and (b), respectively. As for Re $V_{\rm eff}$, the double-well structure is modified into the single-well one when $\mathcal{E}$ increases, so that one can see the phase transition from the NG phase to the WW phase. One also finds that Re $V_{\rm eff}$ has two minima in the chiral limit, while only one absolute minimum exists in the empirical case due to the explicit chiral-symmetry breaking. The value of Im $V_{\rm eff}$ grows up monotonically as $\mathcal{E}$ goes high, and it becomes large for the small $|\bar{M}|$ at the fixed value of $\mathcal{E}$.

As is noted in § 2, σ_J is not simply proportional to $\langle\bar{q}q\rangle_J$ in the presence of the source J_σ except for the extrema of Re $V_{\rm eff}$, where J_σ vanishes,

$$J_\sigma=\frac{\partial}{\partial\sigma}\mathrm{Re}\,V_{\rm eff}\,. \tag{3·5}$$

Figure 3 shows the variation of the source J_σ in the absence of the color-EM field. Such a behavior is qualitatively unchanged even in the presence of the color-EM field.

In this case, the Dyson equation reads

$$\bar{M}_D=\bar{m}+\bar{M}_D\frac{N_f g_{\rm NJL}}{2\pi^2}N_c\int_{1/\Lambda^2}^{\infty}\frac{ds}{s^2}e^{-s\bar{M}_D{}^2}$$

$$-\bar{M}_D\frac{N_f g_{\rm NJL}}{2\pi^2}\frac{\mathcal{E}}{3}\left[F^{\rm fermion}_{\mathcal{E}/(3\Lambda^2)}\left(\sqrt{\frac{3}{\mathcal{E}}}\bar{M}_D,\frac{\pi}{2}\right)+F^{\rm fermion}_{\mathcal{E}/(6\Lambda^2)}\left(\sqrt{\frac{6}{\mathcal{E}}}\bar{M}_D,\frac{\pi}{2}\right)\right]. \tag{3·6}$$

Then the numerical result for the dynamical quark mass $\bar{M}_D$ is shown in Fig. 4. In the u, d-quark sector, the quark condensate $\langle\bar{q}q\rangle$, the order parameter of chiral symmetry, is almost proportional to the dynamical mass $\bar{M}_D$, because the current mass $\bar{m}$ is small. One finds that the dynamical quark mass decreases as $\mathcal{E}$ increases, and its

rapid reduction occurs around $\mathcal{E}=4$ GeV/fm. In the chiral limit, the exact chiral-symmetry restoration takes place at the critical color-electric field, which can be obtained by way of Eq. (2·24),

$$\mathcal{E}_{\rm cr} \simeq \frac{3}{\pi}\left(N_{\rm cr}\Lambda^2 - \frac{2\pi^2}{N_f g_{\rm NJL}}\right) \simeq 4.1\ {\rm GeV/fm}\,. \qquad (3\cdot7)$$

In the chiral limit, the order parameter $\langle\bar{q}q\rangle$ is continuous and a singular point appears, so that the phase transition is second order. On the contrary, there is no clear singular point in the empirical case, so that *mathematically* there seems to be no phase transition.*) However, from the *physical* point of view, one can say that there substantially occurs the chiral-symmetry phase transition even in the empirical case because the order parameter decreases very rapidly about $\mathcal{E}\sim 4$ GeV/fm, which in turn indicates the critical strength $\mathcal{E}_{\rm cr}$ of the chiral-symmetry restoration. We can physically interpret this chiral-symmetry restoration in the strong color-electric field as follows: since quarks and antiquarks in $\langle\bar{q}q\rangle$ have opposite color-charges, q-$\bar{q}$ pairs are pulled apart and consequently the quark condensate $\langle\bar{q}q\rangle$ is broken by the external color-electric field.

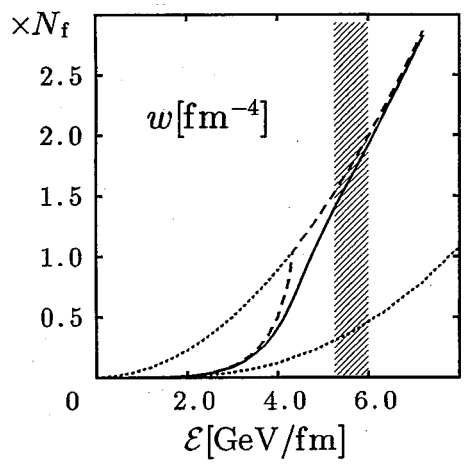

Fig. 5. The q-$\bar{q}$ pair creation rate per unit space-time volume, w, as a function of $\mathcal{E}$ taking account of the variation of the dynamical quark mass. (i) The empirical case ($\bar{m}=5.5$ MeV) and (ii) the chiral limit ($\bar{m}=0$) are expressed by the solid and dashed solid line, respectively. The upper and lower dotted-lines denote the constant cases of "$\bar{M}=0$" and "$\bar{M}=335$ MeV" for any value of $\mathcal{E}$, respectively. The meaning of the shaded region is the same as in Fig. 4.

One also obtains the q-$\bar{q}$ pair creation rate by way of Eq. (3·2),

$$w(\bar{M}) = \frac{N_f}{4\pi^3}\sum_{n=1}^{\infty}\frac{1}{n^2}\left[\left(\frac{\mathcal{E}}{3}\right)^2\exp\left(-\frac{3}{\mathcal{E}}\bar{M}^2 n\pi\right)+2\left(\frac{\mathcal{E}}{6}\right)^2\exp\left(-\frac{6}{\mathcal{E}}\bar{M}^2 n\pi\right)\right], \qquad (3\cdot8)$$

which is simply reduced to $w=N_f\mathcal{E}^2/(144\pi)$ for the massless limit $\bar{M}\to 0$. Figure 5 shows $w(\bar{M}_D)$ as a function of $\mathcal{E}$ using the dynamical quark mass, which is determined by Eq. (3·6). The empirical case ($\bar{m}=5.5$ MeV) and the chiral limit ($\bar{m}=0$) are expressed by the solid and dashed lines, respectively. For comparison, we have added w for the constant mass, $\bar{M}=0$ and $\bar{M}=335$ MeV, denoted by the broken and the dotted lines, respectively. The rate w is largely enhanced in accordance with the reduction of the quark mass around $\mathcal{E}_{\rm cr}$.

§ 4. Extension to the three-flavor case

In this section, we extend our theory to the three-flavor case, including the

*) In general, there is no definite phase transition or well-defined order parameter in the presence of the explicit symmetry breaking.

s-quark. A natural extension of the formulation in § 3 is possible. The three-flavor NJL Lagrangian can be written in a simplified form,

$$\mathcal{L}=\bar{q}(i\not{D}-m)q+g_{\rm NJL}\sum_{a=0}^{8}\{(\bar{q}\lambda^a q)^2+(\bar{q}i\gamma_5\lambda^a q)^2\}-\frac{1}{2}{\rm tr}_c(\mathcal{F}_{\mu\nu}\mathcal{F}^{\mu\nu})\,, \tag{4·1}$$

where $m={\rm diag}(\bar{m}, \bar{m}, m_s)_f$ is the current-mass matrix, $\lambda^0=\sqrt{2/3}\,{\rm diag}\,(1, 1, 1)_f$ obeying the convention such that ${\rm tr}(\lambda^a\lambda^b)=2\delta^{ab}$.

Using the auxiliary fields σ^a, $\pi^a(a=0, 1, \cdots, 8)$, and integrating out the quark degrees of freedom, one obtains the effective Lagrangian in the mean-field approximation,

$$\mathcal{L}_{\rm eff}=-\frac{1}{4g_{\rm NJL}}\sum_{a=0}^{8}(\sigma^a\sigma^a+\pi^a\pi^a)-i{\rm Tr}\,\ln[i\not{D}-M-\sum_{a=0}^{8}i\gamma_5\lambda^a\pi^a+i\epsilon]\,, \tag{4·2}$$

where M is the dynamical mass *matrix* in the three-flavor case,

$$M=m+\sum_{a=0}^{8}\lambda^a\sigma^a\,. \tag{4·3}$$

Since the mass matrix is diagonalized in the physical vacuum that is parity eigenstate, only σ^0, σ^3 and σ^8 have non-vanishing expectation values; in our treatment, the small difference between the u, d-quark mass is neglected, so that σ^3 should also vanish. Then the dynamical mass matrix M in the three-flavor case is reduced to the diagonal form, ${\rm diag}(\bar{M}, \bar{M}, M_s)_f$, where $\bar{M}$ and M_s are given by

$$\bar{M}=\bar{m}+\sqrt{\frac{2}{3}}\sigma^0+\frac{1}{\sqrt{3}}\sigma^8\,,\quad M_s=m_s+\sqrt{\frac{2}{3}}\sigma^0-\frac{2}{\sqrt{3}}\sigma^8\,. \tag{4·4}$$

Then the effective Lagrangian is obtained

$$\begin{aligned}\mathcal{L}_{\rm eff}=&-\frac{(\bar{M}-\bar{m})^2}{4g_{\rm NJL}}-2i{\rm Tr}^*\ln[i\not{D}-\bar{M}+i\epsilon]\\&-\frac{(M_s-m_s)^2}{8g_{\rm NJL}}-i{\rm Tr}^*\ln[i\not{D}-M_s+i\epsilon]\,,\end{aligned} \tag{4·5}$$

where Tr* denotes the functional trace without the flavor degrees of freedom. In this equation, the s-quark sector is completely decoupled from the u, d-quark sector, and its form is the same as that of u- or d-quarks except its mass, which is the same form as in the $SU(2)_f$ case, Eq. (2·6). Hence the results in the previous chapters can be applied: its real part reads

$$\begin{aligned}{\rm Re}\mathcal{L}_{\rm eff}=&-\frac{(\bar{M}-\bar{m})^2}{4g_{\rm NJL}}-\frac{(M_s-m_s)^2}{8g_{\rm NJL}}\\&+\frac{1}{4\pi^2}{\rm tr}_c{\rm pv}\int_{1/\Lambda^2}^{\infty}\frac{ds}{s^3}e^{-s\bar{M}^2}(gHs){\rm coth}(gHs)\cdot(gEs){\rm cot}(gEs)\\&+\frac{1}{8\pi^2}{\rm tr}_c{\rm pv}\int_{1/\Lambda^2}^{\infty}\frac{ds}{s^3}e^{-sM_s^2}(gHs){\rm coth}(gHs)\cdot(gEs){\rm cot}(gEs);\end{aligned} \tag{4·6}$$

its imaginary part is given by

$$\mathrm{Im}\mathcal{L}_{\mathrm{eff}}=-\mathrm{Im}\,V_{\mathrm{eff}}$$

$$=\frac{1}{4\pi^2}\mathrm{tr}_c\sum_{n=1}^{\infty}\frac{gH\cdot gE}{n}\coth(HE^{-1}n\pi)\exp\{-n\pi\bar{M}^2/(gE)\}$$

$$+\frac{1}{8\pi^2}\mathrm{tr}_c\sum_{n=1}^{\infty}\frac{gH\cdot gE}{n}\coth(HE^{-1}n\pi)\exp\{-n\pi\bar{M}_s^2/(gE)\}\,. \qquad (4\cdot7)$$

By putting the extremum conditions on $\mathrm{Re}\,V_{\mathrm{eff}}$ with respect to $\bar{M}$ and M_s, the Dyson equations for $u(d)$ and s-quark can be obtained, respectively. For the u, d-quark sector, the Dyson equation in § 2 holds, while that for the s-quark is given by

$$M_s=m_s+\frac{g_{\mathrm{NJL}}}{\pi^2}M_s\mathrm{tr}_c\mathrm{pv}\int_{1/\Lambda^2}^{\infty}\frac{ds}{s^2}e^{-sM_s^2}(gEs)\cot(gEs)\cdot(gHs)\coth(gHs)\,, \qquad (4\cdot8)$$

which is reduced to the expression for the u, d-quark by replacing m_s, M_s by $\bar{m}$, $\bar{M}$.

The q-$\bar{q}$ pair creation rate w is derived from the imaginary part of $\mathcal{L}_{\mathrm{eff}}$, $w=2\mathrm{Im}\mathcal{L}_{\mathrm{eff}}$, as in Eq. (2·27). In terms of the individual flavors, w consists of three terms,

$$w=w_u+w_d+w_s\,, \qquad (4\cdot9)$$

where w_u denotes u-$\bar{u}$ pair creation etc. Of course w_u+w_d coincides with w in Eq. (2·27) by way of $w_u=w_d$. The s-$\bar{s}$ pair creation rate is given by

$$w_s=\frac{1}{4\pi^2}\mathrm{tr}_c\sum_{n=1}^{\infty}\frac{gH\cdot gE}{n}\coth(HE^{-1}n\pi)\exp\{-n\pi M_s^2/(gE)\}\,. \qquad (4\cdot10)$$

The parameters, g_{NJL} and Λ, can be chosen to be the same as in § 3 because the Dyson equation is unchanged for u, d-quark (see condition (3·3)). We take the current mass of s-quark as the empirical value, $m_s=150$ MeV. Then its dynamical mass becomes 505 MeV in the absence of the external field; such a value is quite reasonable as the constituent quark mass of s-quark.

The dynamical mass of s-quark is also shown in Fig. 4. They vary moderately with respect to $\mathcal{E}$ for s-quark compared with that of u, d-quark: the large explicit breaking of chiral symmetry tends to smear out the decrease of the order parameter.*)

Thus, as a remarkable feature, the strange condensate $\langle\bar{s}s\rangle$ remains to take a rather *large* value even above the critical field strength $\mathcal{E}_{\mathrm{cr}}\simeq4$ GeV/fm, where the chiral-symmetry restoration may take place in the $SU(2)_f$ case. Hence large s-quark mass may be expected even in the WW phase brought by the strong color-electric field.**) The s-$\bar{s}$ pair creation rate in the external color-electric field is shown in Fig. 6. We find that the value of w_s is much smaller than w_u due to large value of the s-quark mass. We also see the small variation of w_s with respect to $\mathcal{E}$.

*) Such a tendency was also shown for the u, d-quark sector in § 5 by comparing the "empirical case" ($\bar{m}=5.5$ MeV) and the chiral limit ($\bar{m}=0$).

**) Such a tendency at high temperature has been also indicated: a large value of $\langle\bar{s}s\rangle$ remains above the critical temperature.[27]

§ 5. Comparison with another approach

In recent papers, Klevansky and Lemmer have taken somehow different approach in a similar context,[11] which corresponds to the constrained Hartree approximation (CHA).[28] The effective potential approach and their CHA approach should be the same within the mean-field approximation, that we have used in the previous sections. However, in spite of their apparent similarities, two basic differences exist between them: one is in the introduction of the source term, and the other is in the use of the field equation. In this section, we figure out these two differences and clarify the mutual relationship for two-flavor case, which may be easily extended to the three-flavor case.

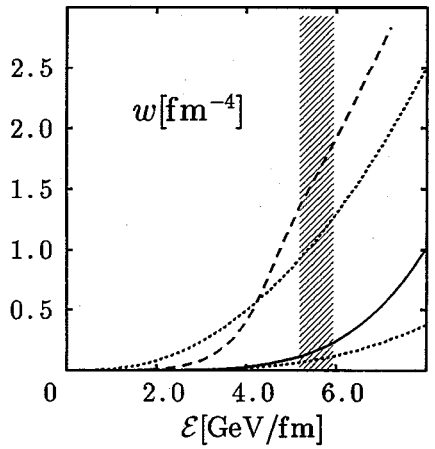

Fig. 6. The s-$\bar{s}$ pair creation rate per unit space-time volume, w_s, as a function of $\mathcal{E}$ taking into account the variation of the dynamical quark mass. The upper and lower dotted lines denote the constant cases of "M_s=150 MeV" and "M_s=505 MeV" for any value of $\mathcal{E}$, respectively. The dashed line denotes the pair creation rate for u, d-quark, w_u. The meaning of the shaded region is the same as in Fig. 4.

We have used the path-integral formalism with respect to auxiliary fields, where the source terms are simply introduced as $J_\sigma\sigma$, $\boldsymbol{J}_\pi\cdot\boldsymbol{\pi}$. However, one can introduce another type of the source term composed of $\bar{q}$ and q,[29] which is used in the CHA approach,

$$\mathcal{Z}[\lambda_S, \boldsymbol{\lambda}_P]=\int DqD\bar{q}\exp\Big[i\int d^4x\{\mathcal{L}_{\mathrm{NJL}}+gj_\mu{}^a G^{\mu a}+\lambda_S\bar{q}q+\boldsymbol{\lambda}_P\cdot\bar{q}\gamma_5\boldsymbol{\tau}q\}\Big]. \tag{5·1}$$

We note that the quark condensate $\langle\bar{q}q\rangle_\lambda$ is derived directly from Eq. (5·1),

$$\langle\bar{q}q\rangle_\lambda=\frac{1}{i\mathcal{Z}}\frac{\delta\mathcal{Z}}{\delta\lambda_S} \tag{5·2}$$

in this case in contrast with Eq. (2·5). By way of the proper-time method, Eq.(5·2) leads to the "gap relation",[11] which is nothing but the usual gap equation in the presence of the source term,

$$\langle\bar{q}q\rangle_\lambda=-\frac{N_f}{4\pi^2}\bar{M}\mathrm{tr}_c\mathrm{pv}\int_{1/\Lambda^2}^{\infty}\frac{ds}{s^2}e^{-s\bar{M}^2}(gHs)\coth(gHs)\cdot(gEs)\cot(gEs), \tag{5·3}$$

where $\bar{M}=\bar{m}-2g_{\mathrm{NJL}}\langle\bar{q}q\rangle_\lambda-\lambda_S$ is the dynamical mass in the presence of the source term. The effective potential ${}^{\mathcal{C}}V_{\mathrm{eff}}$ can be also derived in the same way as V_{eff} in the previous sections,

$${}^{\mathcal{C}}V_{\mathrm{eff}}=V_{\mathrm{eff}}-\frac{1}{4g_{\mathrm{NJL}}}(\lambda_S{}^2+\boldsymbol{\lambda}_P{}^2). \tag{5·4}$$

Since two kinds of the effective potential take the same values at their extrema, which

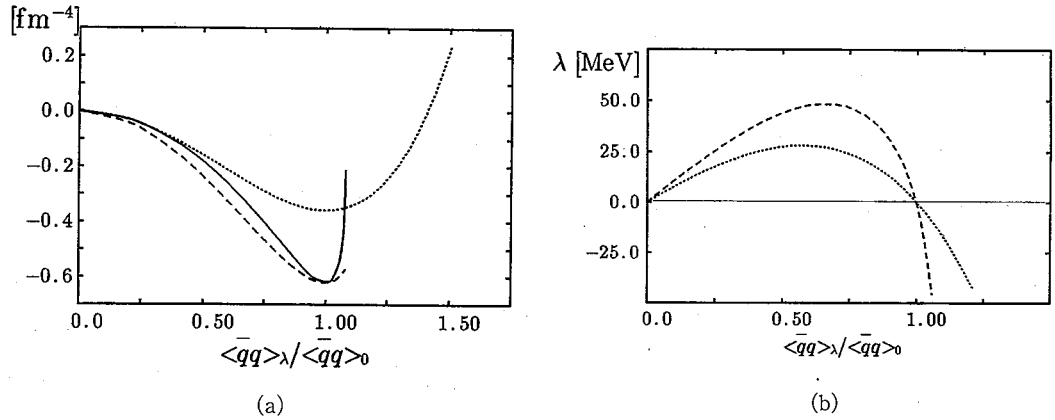

Fig. 7. (a) Effective potentials obtained by three different approaches in the absence of the color-EM field: the solid and dashed lines show $V_{\rm eff}$ and ${}^{CV}V_{\rm eff}$ obtained by way of the effective potential approach, respectively. The dotted line is calculated by using the constrained Hartree approximation (CHA). The horizontal axis is $\langle\bar{q}q\rangle_\lambda/\langle\bar{q}q\rangle_0$. In the effective potential approach, no solution can be obtained for $|\langle\bar{q}q\rangle_\lambda|>1.1\cdot|\langle\bar{q}q\rangle_0|$. The origin in the vertical axis has been taken suitably. (b) The variation of the source λ_S as a function of $\langle\bar{q}q\rangle_\lambda/\langle\bar{q}q\rangle_0$: the dashed and dotted lines are obtained by the effective potential approach and CHA, respectively.

correspond to the physical vacuum with $\lambda_S=\lambda_P=0$, the Dyson equation (2·20) and the q-$\bar{q}$ pair creation rate (2·27) remain unchanged.

Numerical results for the real part of the effective potential are shown in Fig. 7(a), where the horizontal axis denotes the variation of the quark condensate $\langle\bar{q}q\rangle_\lambda/\langle\bar{q}q\rangle_0$ ($\langle\bar{q}q\rangle_0=-2\cdot(250\,\mathrm{MeV})^3$); the values of λ_S and J_σ are shown in Fig. 7(b). One can see the solid and dashed lines, the results of the effective potential approach, are terminated at $|\langle\bar{q}q\rangle_\lambda|\simeq 1.1\cdot|\langle\bar{q}q\rangle_0|$. This is because the gap relation (5·3) does not have any solution for $|\langle\bar{q}q\rangle_\lambda|>1.1\cdot|\langle\bar{q}q\rangle_0|$, although M takes arbitrary value as λ_S varies.

Next we consider the use of the field equation for the quark field, which is derived from the Lagrangian $\mathcal{L}$ in Eq. (2·1),

$$(i\partial\!\!\!/-\bar{m})q^a+2g_{\rm NJL}[(\bar{q}q)q^a+(\bar{q}i\gamma_5\boldsymbol{\tau}q)(i\gamma_5\boldsymbol{\tau}q)^a]=0 \tag{5·5}$$

or

$$\bar{q}(i\partial\!\!\!/-\bar{m})q+2g_{\rm NJL}[(\bar{q}q)^2+(\bar{q}i\gamma_5\boldsymbol{\tau}q)^2]=0\,. \tag{5·6}$$

One may replace the four-fermion interaction term by the bilinear term in the energy-momentum tensor by way of this equation, as Klevansky and Lemmer have done.[11] However Eq. (5·6) is *not trivial* in non-renormalizable theories. Suppose that we take the expectation value of Eq. (5·6) and simply regularize it by way of the proper-time method with cutoff η, then the result may read

$$\frac{N_fN_c}{8\pi^2}\int_\eta^\infty\frac{ds}{s^3}e^{-s\bar{M}^2}+\frac{N_fN_c}{4\pi^2}\bar{m}\bar{M}\int_\eta^\infty\frac{ds}{s^2}e^{-s\bar{M}^2}+2g_{\rm NJL}[\langle(\bar{q}q)^2\rangle+\langle(\bar{q}i\gamma_5\boldsymbol{\tau}q)^2\rangle]=0 \tag{5·7}$$

in the absence of the external gauge field. Since all terms on the left-hand side of Eq. (5·7) are positive, one should not use this equation as it is.*) Klevansky and Lemmer seem to use a similar equation in Ref. 11). To make this equation well-defined, one should *properly* use the regularization scheme. On the other hand, we have never used the field equation in the effective potential approach.

The comparison between the two approaches is also shown in Fig. 7; the dashed lines in Figs. 7(a) and (b) show the total energy and the source λ_S obtained by the CHA approach in the absence of external fields, respectively. The parameters are fixed such that $\langle\bar{q}q\rangle=-(250\text{ MeV})^3$, $\bar{M}=335$ MeV at the minimum. Two results are quite similar qualitatively for both the total energy and the source parameter. Even in the presence of the external color-EM field, the large difference would not be seen between them. Little discrepancy appeared here originates from the fact that the NJL model is not renormalizable, while both should give completely the same results in the renormalizable theories.

However, Klevansky et al. did not deal with q-$\bar{q}$ pair creation in their framework of CHA. On the contrary, both chiral symmetry and q-$\bar{q}$ pair creation can be studied simultaneously in the effective potential approach.

§ 6. Further discussion

—— Application to the flux-tube picture ——

In QCD, the color-electric field is expected to be squeezed into the string-like tube due to the self-interaction of the gluon field: some lattice simulations have shown the flux-tube formation.[30] Then we try to extract physical consequences from our results with the help of the flux-tube picture. We model this picture as follows: the flux tube has the sharp boundary that encloses the deconfinement region**) in the QCD vacuum, and has a constant cross section, S. The color-EM field between valence quarks can only exist inside the flux tubes and is *covariantly constant* within the static approximation, where valence quarks or antiquarks do not change their color, so that only diagonal parts, G_μ^3 and G_μ^8, can contribute. Hence previous formulation can be applied to the system inside the flux tubes. The Gauss laws are valid for the two kinds of "charge" independently, $Q_A=E_AS$ and $Q_B=E_BS$, within the same approximation. Hence, the color-electric field in the tubes formed by quarks is given by $E=\text{diag}(g/3S, g/6S, g/6S)_c$ etc. so that one finds $\mathcal{E}=g^2/S$.

6.1. *Hadron structure*

The color flux-tube model is one of the most popular models in studying the hadron reaction and its structure.[19] In this picture, hadrons consist of color charges (sources) and the color flux-tubes between them: valence quarks and/or antiquarks provide the color sources, and the color flux-tubes are formed by them. Such a picture is typically applicable for mesons, which are considered to be bound states of the valence quark and antiquark. As for baryon, it has been often regarded as the bound state of the valence quark and the *di-quark;* the diquark corresponds to a

*) Equation (5·7) leads to the gap relation, if one carries out the partial integration for the first term of Eq. (5·7) and neglect the surface term, which should diverge originally when $\eta=0$.

**) This can be considered as the intermediate region.

cluster of two valence quarks, and ordinary obeys the 3* representation like the antiquark in the $SU(3)_c$. Such a picture for baryons has been taken not only for highly-excited baryons in the high-energy experiment, but also for the structure of low-lyng baryons.[31] Therefore similar formulae can be applicable for both mesons and baryons in the flux-tube picture by regarding baryon as the binding system of quark and the di-quark.

The string tension k, the energy per unit length, is written as

$$k=\frac{1}{2}(E_A{}^2+E_B{}^2)S=\frac{1}{2S}(Q_A{}^2+Q_B{}^2)=\frac{g^2}{6S} \tag{6·1}$$

by way of the Gauss law. Then the color-electric field inside the hadron flux-tube can be estimated as $\mathcal{E}=5.3\sim6.0[\mathrm{GeV/fm}]>\mathcal{E}_{\mathrm{cr}}$ using the "empirical" value of the string tension $k=0.89\sim1.0[\mathrm{GeV/fm}]$, which is derived from the Regge slope.[19] Therefore chiral symmetry would be restored inside hadrons, which may suggest the chiral bag picture[3] for hadrons: chiral symmetry is restored in their interior by a strong color-electric field, while it is spontaneously broken in their exterior region, where no color-electric field exists.

Finally, it may be worth mentioning the color confinement in our framework. As is well-known, string tension k is one of the most important quantities for the color confinement; string tension k corresponds to the gradient of the linear static potential between quark and antiquark, so that k or $\mathcal{E}=6k$ measures the "strength" of the color-confinement. Then variation of $\mathcal{E}$ is interpreteted as that of the confining force, which would be brought by some nonperturbative effects of gluons like $\langle\mathcal{F}_{\mu\nu}\mathcal{F}^{\mu\nu}\rangle$ or the "monopole condensation" á la 't Hooft.[25] Our results indicate the following. As the confining force grows strong, the color flux is strongly squeezed and vice versa. For the former case, chiral symmetry is restored due to the strong color-electric field, while it is still broken inside the flux tube for the latter case. From the analysis of the Regge trajectory, the value of $\mathcal{E}$ seems larger than $\mathcal{E}_{\mathrm{cr}}$ inside hadrons, so that the former case would be realized in the nature. Of course, the physical value of k should be derived from the theoretical framework endowed with the confinement mechanism. To this end, further efforts are needed for understanding color confinement.

6.2. *Ultrarelativistic heavy-ion collisions*

The flux-tube picture has been also popular in the studies of QGP formation in ultrarelativistic heavy-ion collisions.[19),32] After the collision, QGP formation would be supposed to occur through the following two stages.

(1) Pre-equilibrium stage; immediately after the collision, many color flux-tubes are formed between heavy ions, which may give a strong color field. Then, by the Schwinger mechanism, q-$\bar{q}$ pair creation violently occurs inside tubes. During this process, the color field is weakened, on the contrary, the thermal energy grows up, so that the energy of the color-EM field turns into the thermal one: the energy is thus deposited.

(2) QGP formation; a *hot* QGP, which is regarded to be a equilibrium system, may be formed in the central region for sufficiently high-energy collisions. In this stage

there is no more external color field.

So far, many studies have been devoted mainly to the equilibrium stage (2), while, the pre-equilibrium stage (1) has been also studied in recent years with much interest.[6] Our study can be closely related to the stage (1), because only the color external field may exist in this situation, which is rather similar to the hadron in the flux-tube picture. These flux tubes may be formed by piling up such ones as in the hadron, and one can expect a stronger color-electric field ($\mathcal{E} \sim$several GeV/fm) in the flux tubes, so that chiral symmetry would be restored there. This conjecture would affect the q-$\bar{q}$ pair creation rate. The energy of the color field turns into the thermal one through q-$\bar{q}$ pair creations, which strongly depend on the quark mass (see Fig. 5). If the system remains in the NG phase, the constituent quark mass is relevant, then this creation rate becomes rather small. On the contrary, if the phase transition of chiral symmetry takes place due to the strong color-electric field, the current quark mass should be applied, so that one can expect a larger q-$\bar{q}$ pair creation rate. Our study suggests that manifestation of chiral symmetry is changed from the NG phase to the WW phase during the pre-equilibrium stage (1), so that the current quark mass seems to be suitable on calculating the q-$\bar{q}$ pair creation rate. Experimentally, such a phase transition may affect the cross section of dilepton production or direct gamma emission that stems from q-$\bar{q}$ pair annihilation in the pre-equilibrium stage.

However these consequences for ultrarelativistic heavy-ion collisions may be too simple because some diabatic effects and the finite size effect of the flux tubes[33] have been disregarded. In particular, diabatic effects related to the expansion of the system seem to enhance the q-$\bar{q}$ pair creation rate: the energy of the flux tube is almost proportional to its length, so that the stretched flux tube tends to be unstable against q-$\bar{q}$ pair creation. It deserves more elaborate studies for quantitative arguments.

§ 7. Summary and concluding remarks

We have studied the manifestation of chiral symmetry and q-$\bar{q}$ pair creation in the presence of the external color-EM field, using the NJL model. These two subjects have been simultaneously understood in terms of the effective potential formalism. We have derived the effective potential, the Dyson equation for the dynamical quark mass and the q-$\bar{q}$ pair creation rate in the presence of the external color-EM field that is covariantly constant. As a remarkable fact, since these expressions have been obtained by the full-order treatment of the color-EM field, they include the nonperturbative effects of the color-EM field.

We have applied our formulae to the physical situations of the system around quarks or antiquarks, and have found that the chiral-symmetry restoration would take place by the sufficiently strong color-electric field, and rapid reduction of the quark mass has been found around the critical field strength, $\mathcal{E}_{\rm cr} \simeq 4$ GeV/fm. We have also calculated the q-$\bar{q}$ pair creation rate, and its rapid increasing has been found around the critical field strength due to the rapid reduction of the dynamical quark mass.

Our study suggests that the chiral-symmetry restoration would take place in the

sufficiently strong *color-electric* field. It is rather similar to the phase transition at high temperature. As for the similarity of the effects on chiral symmetry between the color-electric field and temperature, one may be able to understand it by considering how the quark condensate $\langle \bar{q}q \rangle$ disappears; in the external color-electric field, q-$\bar{q}$ pairs are pulled apart and consequently $\langle \bar{q}q \rangle$ is broken; at finite temperature, $\langle \bar{q}q \rangle$ is also broken by the thermal fluctuation. Similar analogy appears in the superconductivity in the presence of the external *magnetic* field or at high temperature. Since the Cooper pair, which consists of two electrons with the opposite spin, is broken by the spin-magnetic interaction or thermal fluctuation, superconductors become normal state in the strong magnetic field or at high temperature. In spite of the difference in the formalism, interesting physical correspondence may be found between the quark condensate in the QCD vacuum and the Cooper pair in the superconductivity, however, there exists large difference on the reaction for the external fields; the latter is broken by the magnetic field, in contrast, the former is not broken by the color-magnetic field but by the color-electric field.

The extension to the three-flavor case has been also done, and the variations of the dynamical mass and the pair creation rate of s-quarks have been rather moderately small in comparison with those of u, d-quarks.

We have compared the effective potential approach with the constrained Hartree one which Klevansky et al. have used. There are two differences between them in terms of the introduction of the source terms or the use of the field equation. However these two approaches give similar results to those for the manifestation of chiral symmetry.

Actual calculation based on the color flux-tube picture has shown that there would be the chirally-symmetric phase in the flux tube inside hadrons. It is interesting that this result may lead to the chiral bag picture for hadrons: the chirally-symmetric phase exists inside the flux tube due to the strong color-electric field, on the contrary chiral symmetry remains broken outside the flux tube, where color fields are absent.

We have also applied our theory to the early stage of ultrarelativistic heavy-ion collisions, and have obtained the conjecture that chiral-symmetry restoration would occur due to the strong electric color-field just after the collisions. For the study of the thermalization, it is quite desirable to formulate the q-$\bar{q}$ pair creation at finite temperature and/or in finite density.[34] Such a subject is, however, very difficult because the (color-)electric field is time component of $\mathcal{F}_{\mu\nu}$ and it is not clear whether we can properly treat it at finite temperature and/or in finite density.

Our theory is based on the "infrared" effective theory of QCD, so that there exists inevitable constraint in applying it to such systems in the strong external field. For instance, the coupling constant of the four-fermion interaction (g_{NJL}) would have the dependence on the external field because it effectively includes the effects of underlying *virtual* gluon fields and quarks, of which dynamics would be altered according to the external fields or temperature of the system. However one can guess that the results here are not changed at least qualitatively, because one can expect that the four-fermion coupling g_{NJL}, which induces the χSB, would be reduced in the strong color-electric field or at high temperature due to the asymptotic behavior of QCD.[15),16)]

Then the actual variation of the dynamical quark mass may be more rapid than the results of the model calculation by way of the NJL model. Hence the value of $\mathcal{E}_{cr}$ would be able to be regarded as *upper limit* of the critical field strength of the chiral-symmetry restoration.

From our study based on the effective model of QCD, we can at least insist on the features on the restoration of chiral symmetry in the strong color-electric field. In order to get deeper insight, it is indispensable to study different approach such as lattice QCD simulations. In Ref. 13), Austrian group has found the reduction of the quark condensate $\langle\bar{q}q\rangle$ around quarks or the color sources by using lattice QCD simulations.

In this paper, we have concentrated on the intermediate region indicated by Manohar and Georgi; there scarcely exist the nonperturbative effects relevant to the color confinement, like the gluon condensation, while those relevant to the χSB may survive there. However the color-confinement mechanism would be also important in some cases, e.g., flux-tube formation. Therefore, further studies are needed to get a consistent description of the confinement and χSB in the low-energy region of QCD. As the first step to this end, we should take into account the modification of such a complicated gluon configuration as being suggested by Savvidy et al.[15] or Copenhagen group[16] in the external color-EM field at the same time. On the other hand, the study of gluon configurations[35] and the quark condensate[13] around color sources should be done at the same time by lattice QCD simulations. Such studies are important and strongly desired in understanding chiral symmetry and/or q-$\bar{q}$-pair creation in the color-EM field.

Acknowledgements

We wish to thank Professor R. Tamagaki for his interest and encouragement. We are also indebted to members of nuclear theory group in Kyoto for useful discussions and especially to Dr. T. Fukui for stimulating discussion about the constrained Hartree approximation. We thank Professor M. Karliner for his interest and correspondence.

Appendix
—— ζ-*function Regularization Method* ——

A.1. *Formalism*

In § 2, we have used the proper-time method with a cutoff Λ to regularize the quark determinant. Here we show that we can formulate our subject by way of the ζ-function regularization, which we have used to analyze the symmetry behavior in QED,[8),17)] and discuss similarities and differences between them. In the ζ-function regularization, the functional determinant of $\hat{O}$ is regularized as

$$\ln \mathrm{Det}\hat{O}=\mathrm{Tr}\ln\hat{O}=\lim_{\nu\to 0}\left[-\frac{d}{d\nu}\mathrm{Tr}\hat{O}^{-\nu}\right]=\lim_{\nu\to 0}\left[-\frac{d}{d\nu}\zeta_{\hat{O}}(\nu)\right], \qquad (\mathrm{A}\cdot 1)$$

where

$$\zeta_{\hat{O}}(\nu)\equiv\frac{1}{\Gamma(\nu)}\int_0^\infty ds\, s^{\nu-1}\mathrm{Tr}\exp(-\hat{O}s)\,. \tag{A·2}$$

Hence, $\mathcal{L}_{\mathrm{loop}}$ in Eq. (2·7) can be expressed as

$$\mathcal{L}_{\mathrm{loop}}=-\frac{i}{2}\lim_{\nu\to 0}\left\{-\frac{d}{d\nu}\left[\frac{i^\nu}{\Gamma(\nu)}\int_0^\infty ds\, s^{\nu-1}\mathrm{tr}\langle x|\exp(-\mathcal{G}^{-1}s)|x\rangle\right]\right\}, \tag{A·3}$$

where $\mathcal{G}$ is derived from the quark propagator in the physical vacuum $\boldsymbol{\pi}=0$,

$$\mathcal{G}^{-1}=i\left[-(\Pi^\mu)^2+\frac{g}{2}\sigma_{\mu\nu}\mathcal{F}^{\mu\nu}_{\mathrm{ex}}+\bar{M}^2-i\epsilon\right]/\mu^2 \tag{A·4}$$

with $\Pi^\mu=i\partial^\mu+gG^\mu_{\mathrm{ex}}$. Here we have introduced an arbitrary parameter μ with the dimension of a mass, which can be regarded as a renormalization point. Here the choice of μ is completely arbitrary: if one takes the different value for μ, the coupling constants in the theory will be merely reparametrized.[36] Then the evaluation of the effective Lagrangian is reduced to the eigenvalue problem for the operators K_X and K_Y.[8]

When the color-EM field is covariantly constant, the integrand in Eq. (A·3) is reduced to the form

$$\begin{aligned}\mathrm{tr}\langle x|\exp(-\mathcal{G}^{-1}s)|x\rangle=4N_f\mathrm{tr}_c\cos\left(\frac{gH}{\mu^2}s\right)\cosh\left(\frac{gE}{\mu^2}s\right)\cdot e^{-is(\bar{M}^2-i\epsilon)/\mu^2}\\ \times\langle xy|\exp\left(-2is\frac{gH}{\mu^2}K_X\right)|xy\rangle\langle tz|\exp\left(-2is\frac{gE}{\mu^2}K_Y\right)|tz\rangle\,;\end{aligned} \tag{A·5}$$

in a suitable Lorentz frame (2·15), where the operator variables K_X and K_Y are defined by

$$K_X=\frac{1}{2}(gH)^{-1}(\Pi_1^2+\Pi_2^2)\,,\quad K_Y=\frac{1}{2}(gE)^{-1}(\Pi_3^2-\Pi_0^2)\,. \tag{A·6}$$

Since K_X is a familiar harmonic-oscillator operator and its eigenvalues are known to be discrete Landau levels, one easily obtains

$$\begin{aligned}\langle xy|\exp\left(-2i\frac{gH}{\mu^2}sK_X\right)|xy\rangle&=\frac{gH}{2\pi}\sum_{n=0}^{\infty}\exp\left[-is\frac{2gH}{\mu^2}\left(n+\frac{1}{2}\right)\right]\\ &=\frac{gH}{4\pi i}\cdot\frac{1}{\sin(gHs/\mu^2)}\,.\end{aligned} \tag{A·7}$$

On the contrary, operator K_Y is an inverted harmonic-oscillator operator; its eigenvalues are continuous and take values from $-\infty$ to ∞, so that the sum over them is rather difficult. However, its eigenfunctions are known to be described by linear combinations of the parabolic cylindrical functions and the state density can be obtained.[37] Hence one can get the similar relation to Eq. (A·7) as

$$\langle tz|\exp\left(-2i\frac{gE}{\mu^2}sK_Y\right)|tz\rangle=\frac{gE}{4\pi}\cdot\frac{1}{\sinh(gEs/\mu^2)} \tag{A·8}$$

besides the irrelevant constant.

By way of Eqs. (A·5), (A·7) and (A·8), one obtains the compact form $\mathcal{L}_{\text{loop}}$ in Eq. (A·3),

$$\begin{aligned}\mathcal{L}_{\text{loop}}=&\frac{N_f}{8\pi^2}\mathrm{tr}_c\lim_{\nu\to 0}\left\{\frac{d}{d\nu}\left[\frac{i^\nu}{\Gamma(\nu)}\right.\right.\\&\left.\left.\times\int_0^\infty ds\, s^{\nu-1}g^2EH\cot\left(\frac{gH}{\mu^2}s\right)\cdot\coth\left(\frac{gE}{\mu^2}s\right)e^{-is(\bar{M}^2-i\epsilon)/\mu^2}\right]\right\}\\=&-\frac{N_f}{8\pi^2}\mathrm{tr}_c\lim_{\nu\to 0}\frac{d}{d\nu}\left[\frac{1}{\Gamma(\nu)}\right.\\&\times\mathrm{pv}\int_0^\infty ds\, s^{\nu-3}(gHs)\coth\left(\frac{gH}{\mu^2}s\right)\cdot(gEs)\cot\left(\frac{gE}{\mu^2}s\right)e^{-s\bar{M}^2/\mu^2}\\&\left.-i\frac{1}{\Gamma(\nu)}\sum_{n=1}^\infty\left(\frac{n\pi\mu^2}{gE}\right)^\nu\frac{gH\cdot gE}{n}\coth(n\pi HE^{-1})e^{-n\pi\bar{M}^2/(gE)}\right],\end{aligned}\tag{A·9}$$

where we have modified the path in the s-plane and changed the integral variable, $s\to -is$. The second term of the RHS in Eq. (A·9) is derived from residues around the poles $s=-n\pi i\mu^2/(gE^{(i)})$ $(i=1, 2, 3;\ n=1, 2, \cdots, \infty)$ in the original s-plane.

Here we separate the "divergent" part at $\nu=0$ in Eq. (A·9) and use the analytical continuation in the complex ν-plane. Then it can be expressed in terms of the generalized Riemann zeta-function and the gamma function.[8] Hence one gets the finite expression for the one-loop effective potential,

$$\begin{aligned}V_{\text{loop}}=-\mathcal{L}_{\text{loop}}=&\frac{N_f}{8\pi^2}\mathrm{tr}_c\mathrm{pv}\int_0^\infty ds s^{-3}e^{-s\bar{M}^2}\\&\times\left[(gEs)\cot(gEs)\cdot(gHs)\coth(gHs)-1-\frac{g^2}{3}(H^2-E^2)s^2\right]\\&-\frac{N_fN_c}{16\pi^2}\left[\bar{M}^4\ln\frac{\bar{M}^2}{\mu^2}-\frac{3}{2}\bar{M}^4\right]-\frac{N_fg^2}{24\pi^2}\ln\frac{\bar{M}^2}{\mu^2}\mathrm{tr}_c(H^2-E^2)\\&-i\frac{N_f}{8\pi^2}\mathrm{tr}_c\sum_{n=1}^\infty\frac{gH\cdot gE}{n}\coth(HE^{-1}n\pi)\exp\{-n\pi\bar{M}^2/(gE)\}\,.\end{aligned}\tag{A·10}$$

Thus we can obtain the *finite* loop contribution without introducing ad hoc cutoff Λ in the proper-time method (see § 2). Although the divergence of the loop integral has been eliminated by way of the ζ-function regularization method, we further need the renormalization procedure, reparametrization of the mass and the coupling constant. In order to obtain the meaningful expression for the effective potential, one must add some *finite* correction subject to the renormalization conditions. We have demonstrated this point by way of the linear σ model in the previous paper.[8] Here we attempt 'renormalization' even for the NJL model within the Hartree approximation, introducing the counter term

$$\delta\mathcal{L}=\delta g_{\text{NJL}}[(\bar{q}q)^2+(\bar{q}i\gamma_5\boldsymbol{\tau}q)^2]-\delta\bar{m}\bar{q}q\,.\tag{A·11}$$

Then the effective potential leads to

$$V_{\rm eff}=\frac{(\bar{M}-\bar{m})^2}{4g_{\rm NJL}}+i{\rm Tr}\,\ln[i\not{D}-\bar{M}+i\epsilon]-\delta g_{\rm NJL}\frac{(\bar{M}-\bar{m})^2}{4g_{\rm NJL}^2}-\delta\bar{m}\frac{\bar{M}-\bar{m}}{2g_{\rm NJL}}. \qquad (A\cdot12)$$

We assume that the counter term ($\delta\mathcal{L}$) is determined by the 'renormalization' conditions,

$$\left.\frac{\partial V_{\rm loop}}{\partial\bar{M}}\right|_{\bar{M}=\mu}=\left.\frac{\partial^2 V_{\rm loop}}{\partial\bar{M}^2}\right|_{\bar{M}=\mu}=0 \qquad (A\cdot13)$$

in the absence of the external field to find

$$\delta g_{\rm NJL}=\frac{N_fN_c}{2\pi^2}g_{\rm NJL}^2\mu^2\,,\quad \delta\bar{m}=\frac{\delta g_{\rm NJL}}{g_{\rm NJL}}\bar{m}\,. \qquad (A\cdot14)$$

Then one obtains a final expression for ${\rm Re}\,V_{\rm eff}$,

$$\begin{aligned}{\rm Re}\,V_{\rm eff}=&\frac{(\bar{M}-\bar{m})^2}{4g_{\rm NJL}}+\frac{N_f}{8\pi^2}{\rm tr}_c{\rm pv}\int_0^\infty ds s^{-3}e^{-s\bar{M}^2}\\&\times\left[(gEs)\cot(gEs)\cdot(gHs)\coth(gHs)-1-\frac{g^2}{3}(H^2-E^2)s^2\right]\\&-\frac{N_fN_c}{16\pi^2}\left[\bar{M}^4\ln\frac{\bar{M}^2}{\mu^2}-\frac{3}{2}M^4+2\mu^2\bar{M}^2\right]-\frac{N_fg^2}{24\pi^2}\ln\frac{\bar{M}^2}{\mu^2}{\rm tr}_c(H^2-E^2)\,. \qquad (A\cdot15)\end{aligned}$$

It is to be noted that there remains only one adjustable parameter $g_{\rm NJL}$ in the final expression apart from the arbitrary scale parameter μ. While in the proper-time method, there are two parameters, $g_{\rm NJL}$ and Λ in Eq. (2·18).

Taking the extrema of ${\rm Re}\,V_{\rm eff}$, one obtains the self-consistent Dyson equation,

$$\begin{aligned}\bar{M}_D=&\bar{m}+\bar{M}_D\frac{N_fN_c}{2\pi^2}g_{\rm NJL}[\bar{M}_D{}^2\ln(\bar{M}_D{}^2/\mu^2)-\bar{M}_D{}^2+\mu^2]\\&+\bar{M}_D\frac{N_fg_{\rm NJL}}{2\pi^2}{\rm tr}_c{\rm pv}\int_0^\infty\frac{ds}{s^2}e^{-s\bar{M}_D{}^2}[(gEs)\cot(gEs)\cdot(gHs)\coth(gHs)-1]\,, \qquad (A\cdot16)\end{aligned}$$

where $\bar{M}_D$ is the dynamical quark mass in the physical vacuum with the external color-EM field. The q-$\bar{q}$ pair creation rate is derived from ${\rm Im}\,V_{\rm eff}$, and has the same form as Eq. (2·27) in § 2.

A.2. *Numerical example*

The effective potential $V_{\rm eff}$ for a given color quark reads

$$\begin{aligned}{\rm Re}\,V_{\rm eff}=&\frac{(\bar{M}-\bar{m})^2}{4g_{\rm NJL}}-\frac{N_fN_c}{16\pi^2}\left[\bar{M}^4\ln\frac{\bar{M}^2}{\mu^2}-\frac{3}{2}\bar{M}^4+2\mu^2\bar{M}^2\right]+\frac{N_f\mathcal{E}^2}{144\pi^2}\ln\frac{\bar{M}^2}{\mu^2}\\&+\frac{N_f}{8\pi^2}{\rm pv}\int_0^\infty\frac{ds}{s^3}e^{-s\bar{M}^2}\left\{\left[\left(\frac{\mathcal{E}}{3}s\right)\cot\left(\frac{\mathcal{E}}{3}s\right)-1\right]\right.\\&\left.+2\left[\left(\frac{\mathcal{E}}{6}s\right)\cot\left(\frac{\mathcal{E}}{6}s\right)-1\right]+\frac{\mathcal{E}^2s^2}{18}\right\},\\{\rm Im}\,V_{\rm eff}=&-\frac{N_f}{8\pi^3}\sum_{n=1}^\infty\frac{1}{n^2}\left[\left(\frac{\mathcal{E}}{3}\right)^2\exp\left(-\frac{3}{\mathcal{E}}\bar{M}^2n\pi\right)+2\left(\frac{\mathcal{E}}{6}\right)^2\exp\left(-\frac{6}{\mathcal{E}}\bar{M}^2n\pi\right)\right],\end{aligned} \qquad (A\cdot17)$$

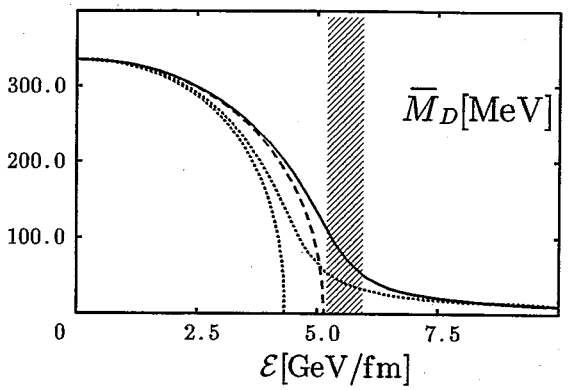

Fig. 8. The dynamical quark mass $\bar{M}_D$ calculated by using the ζ-function regularization method: the solid and dashed lines correspond to the empirical case and the chiral limit, respectively. The dotted lines denote the previous results obtained by way of the proper-time method (Fig. 4). The meaning of the shaded region is the same as in Fig. 4.

similar to Eq. (3·2). In this case, the Dyson equation leads to

$$\bar{M}_D=\bar{m}+\bar{M}_D\frac{N_fN_c}{2\pi^2}g_{\rm NJL}\left[\bar{M}_D{}^2\ln\frac{\bar{M}_D{}^2}{\mu^2}-\bar{M}_D{}^2+\mu^2\right]$$

$$-\bar{M}_D\frac{N_fg_{\rm NJL}}{2\pi^2}\frac{\mathcal{E}}{3}\left[F^{\rm fermion}\left(\sqrt{\frac{3}{\mathcal{E}}}\bar{M}_D,\frac{\pi}{2}\right)+F^{\rm fermion}\left(\sqrt{\frac{6}{\mathcal{E}}}\bar{M}_D,\frac{\pi}{2}\right)\right], \qquad (A\cdot18)$$

where $F^{\rm fermion}(x,\theta)$ is a characteristic function (2·23) (as for the q-$\bar{q}$ pair creation rate w, Eq. (3·8) remains valid).

The scale parameter μ is set as 1 GeV, which corresponds to the typical energy scale of hadron physics, and the remaining parameter $g_{\rm NJL}$ is chosen to give $\bar{M}_D=335$ MeV (the constituent quark mass) in the absence of the external field:

(i) the empirical case ($\bar{m}=5.5$ MeV): $g_{\rm NJL}=0.2015$ fm^2.
(ii) the chiral limit ($\bar{m}=0$): $g_{\rm NJL}=0.205$ fm^2.

In both cases, one can obtain the reasonable value for the quark condensate with *only one* adjustable parameter $g_{\rm NJL}$: one finds $\langle\bar{u}u\rangle\simeq-(254\ {\rm MeV})^3$ in the absence of the external field (cf. Eq. (3·3)).

Then the numerical results of the variations of the dynamical quark mass $\bar{M}_D$ is shown in Fig. 8. In this case, both $\bar{M}_D$ and $\langle\bar{q}q\rangle$ decrease around $\mathcal{E}_{\rm cr}\simeq5$ GeV/fm, so that one can regard this value as the critical field. The empirical case ($m=5.5$ MeV) and the chiral limit ($\bar{m}=0$) are expressed by the solid and dashed lines, respectively. One also finds that the rate w is enhanced around $\mathcal{E}_{cr}$ due to the decrease of the quark mass. Thus one does not find the large differeince from the results in § 3.

References

1) A. Manohar and H. Georgi, Nucl. Phys. **B234** (1984), 189.
G. S. Adkins, C. R. Nappi and E. Witten, Nucl. Phys. **B228** (1983), 552.
H. B. Nielsen and A. Patkos, Nucl. Phys. **B195** (1982), 137.
2) A. Dhar and S. R. Wadia, Phys. Rev. Lett. **52** (1984), 959.

T. Hatsuda and T. Kunihiro, Prog. Theor. Phys. Suppl. No. 91 (1987), 284.
S. P. Klevansky, Rev. Mod. Phys. **64** (1992), 1 and references cited therein.
3) V. Vento, M. Rho, E. M. Nyman, J. H. Jun and G. E. Brown, Nucl. Phys. **A345** (1980), 413.
A. Chodos and C. B. Thorn, Phys. Rev. **D12** (1975), 2733.
T. Inoue and T. Maskawa, Prog. Theor. Phys. **54** (1975), 1833.
4) B. Petersson, Nucl. Phys. **A525** (1991), 237c and references cited therein.
5) A. Barducci, R. Casalbuoni, S. De Curtis, R. Gatto and G. Pettini, Phys. Rev. **D41** (1990), 1610.
6) For instance, papers in Proc. of "Quark Matter '90", Menton, Nucl. Phys. **A525** (1991), 1.
7) T. D. Lee and M. Margulies, Phys. Rev. **D11** (1975), 1591.
8) H. Suganuma and T. Tatsumi, Ann. of Phys. **208** (1991), 470.
9) H. Suganuma and T. Tatsumi, Phys. Lett. **B269** (1991), 371.
10) H. Suganuma and T. Tatsumi, *Proc. of Int. Sympo. on "High Energy Nuclear Collisions and Quark Gluon Plasma", Kyoto,* 6-8 *June* 1991 (World Scientific, Singapore, 1992); preprint KUNS1049; *Proc. of Int. Workshop on "High Density Nuclear Matter", KEK,* 18-21 *Sep.* 1990, to be published.
11) S. P. Klevansky and R. H. Lemmer, Phys. Rev. **D39** (1989), 3478.
12) S. P. Klevansky, J. Jaenicke and R. H. Lemmer, Phys. Rev. **D43** (1991), 3040.
13) W. Sakuler, W. Bürger, M. Faber, H. Markum, M. Müller, P. D. Forcrand, A. Nakamura and I. O. Stamatescu, Phys. Lett. **B276** (1992), 155.
W. Bürger, M. Faber, W. Feilmair and H. Markum, Nucl. Phys. **A525** (1991), 581c.
M. Muller, M. Faber, W. Feilmair and H. Markum, Nucl. Phys. **B335** (1990), 502.
14) T. Suzuki, Prog. Theor. Phys. **80** (1988), 929.
S. Maedan and T. Suzuki, Prog. Theor. Phys. **81** (1989), 229.
M. Baker, J. S. Ball and F. Zachariasen, Phys. Rept. **209** (1991), 73; Phys. Rev. **D38** (1988), 1926.
15) S. G. Matinyan and G. K. Savvidy, Nucl. Phys. **B134** (1978), 539.
G. K. Savvidy, Phys. Lett. **B71** (1977), 133.
I. A. Batalin, S. G. Matinyan and G. K. Savvidy, Sov. J. Nucl. Phys. **26** (1977), 214.
16) H. Pagels and E. Tomboulis, Nucl. Phys. **B143** (1978), 485.
N. K. Nielsen and P. Olesen, Nucl. Phys. **B144** (1978), 376.
H. B. Nielsen and P. Olesen, Nucl. Phys. **B160** (1979), 380.
J. Ambjφrn and P. Olesen, Nucl. Phys. **B170** (1980), 60.
17) W. Dittrich and M. Reuter, Lecture Notes in Physics **220** (1985), 244.
18) For instance, A. B. Balantekin, J. E. Seger and S. H. Fricke, Int. J. Mod. Phys. **A6** (1991), 695 and references cited therein.
19) For a recent review article, K. Sailer, Th. Schönfeld, Zs. Schram, A. Schäfer and W. Greiner, J. of Phys. **G17** (1991), 1005.
20) P. H. Cox and A. Yildiz, Phys. Rev. **D32** (1985), 819.
21) W. Greiner, B. Müller and J. Rafelski, *Quantum Electrodynamics of Strong Fields* (Springer-Verlag, Berlin, Heidelberg, 1985).
22) M. R. Brown and M. J. Duff, Phys. Rev. **D11** (1975), 2124.
A. Yildiz and P. H. Cox, Phys. Rev. **D21** (1980), 1095.
M. Claudson, A. Yildiz and P. H. Cox, Phys. Rev. **D22** (1980), 2022.
23) H. Leutwyler, Nucl. Phys. **B129** (1981), 129.
24) K. Huang, *Quarks, Leptons and Gauge Fields* (World Scientific, Singapore, 1982).
25) G. 't Hooft, Nucl. Phys. **B190** (1981), 455.
26) J. Schwinger, Phys. Rev. **82** (1951), 664.
27) T. Kunihiro, Nucl. Phys. **B351** (1991), 593.
28) P. Ring and P. Schuck, *The Nuclear Many-Body Problem* (Springer-Verlag, New York, 1980).
29) D. J. Gross and A. Neveu, Phys. Rev. **D10** (1974), 3235.
30) A. D. Giacomo, M. Maggiore and Š. Olejník, Nucl. Phys. **B347** (1990), 441.
L. D. Debbio, A. D. Giacomo, M. Maggiore and Š. Olejník, Preprint CERN-TH-6282-91, *Proc. of the 25th Int. Symp. on the "Theory of Elementary Particles", Gosen, Germany, Sep.* 1991.
31) A. B. Migdal, S. B. Khokhlachev and V. Yu. Borue, Phys. Lett. **B228** (1989), 167.
A. B. Migdal, JETP Lett. **46** (1987), 322.
32) G. Gatoff, A. K. Kerman and T. Matsui, Phys. Rev. **D36** (1987), 114.
33) C. Martin and D. Vautherin, Phys. Rev. **D38** (1988), 3593.
C. Martin and D. Vautherin, Phys. Rev. **D40** (1989), 1667.
34) A. Chodos, Phys. Rev. **D42** (1990), 2881.
35) S. Hioki, S. Kitahara, S. Kiura, Y. Matsubara, O. Miyamura, S. Ohno and T. Suzuki, Phys. Lett. **B272** (1991), 326.
36) S. Coleman and E. Weinberg, Phys. Rev. **D7** (1973), 1888.
37) G. Barton, Ann. of Phys. **166** (1986), 322.